

# CPT data interpretation for an improved characterization of the paleosol stratigraphy in the Po River Valley, Italy

I. Bertolini, M. Marchi, L. Tonni & G. Gottardi

*DICAM Department, University of Bologna, Italy*

L. Bruno

*Department of Chemical and Geological Sciences, University of Modena, Italy*

A. Amorosi

*Department of Biological, Geological and Environmental Sciences, University of Bologna, Italy*

**ABSTRACT:** Post-depositional phenomena can produce significant changes in the geotechnical properties of soils. Although the identification of the effect of such phenomena on the soil structure may contribute significantly to the interpretation of the soil mechanical behaviour, their characterization is not routinely carried out in practice. In this context, the novel application of paleosol features in the definition of geotechnical stratigraphic models can result in improved characterization of soil deposits in alluvial sites. Sedimentology uses paleosols (i.e. fossil soils with peculiar geologic properties) as markers for stratigraphic correlations in alluvial areas at large scale. This paper outlines the main properties of these geological objects and investigates the strategies for their identification in cone penetration tests (CPT). The analyses are discussed with reference to boreholes and CPTs data in 3 well documented sites in the Po River Valley (Italy). First, sedimentological identification of paleosols from borehole corings is introduced; then, geotechnical interpretation of CPT is carried out on such a basis, showing how poorly developed paleosols (Inceptisols) found in the investigated sites, are difficult to be identified through CPT logs and how they plot in the well-established Robertson's classification charts.

## 1 INTRODUCTION

The Po Plain-Adriatic sea system is an elongated basin originated from the Po River catchment. It consists of a > 7km thick Pliocene - Quaternary sedimentary succession, with a 30m-thick Holocene succession that overlies Late Pleistocene deposits. The Holocene depositional history can be investigated through integrated stratigraphic, sedimentological and paleontological analyses. A total of 22 sedimentary facies, grouped into 5 main depositional systems, have been identified in the Po River catchment (Amorosi et al, 2017).

The present work focuses on three locations in the Po Plain, in Province of Ferrara (Figure 1), characterized by well-drained floodplain deposits, which belong to the alluvial plain depositional system. These deposits consist of different mixtures of clay and silt and show peculiar pedogenetic features: paleosols. The investigation started from the description of three continuous corings EM-S3, EM-S1 and EM-S5, located in Gaibana, Dogato and Ostellato, respectively. Then, three CPTU tests, each one performed in proximity to one coring, were analysed.

The stratal architecture of the Holocene succession of the Po coastal plain in Figure 2 shows the spatial distribution of the facies associations along the investigated section. The Holocene deposits, down to a depth between -10 and -20 m a.s.l, consist predominantly of a thick swamp clay succession that grades distally into

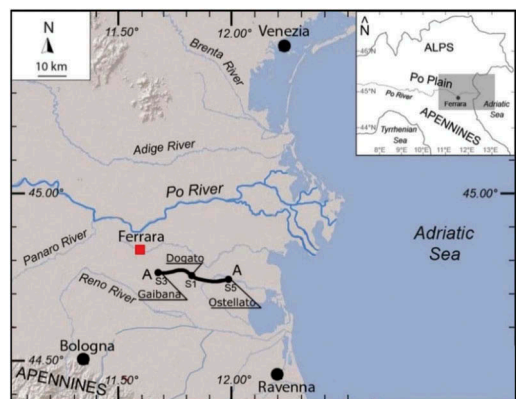


Figure 1. Location of the investigated site.

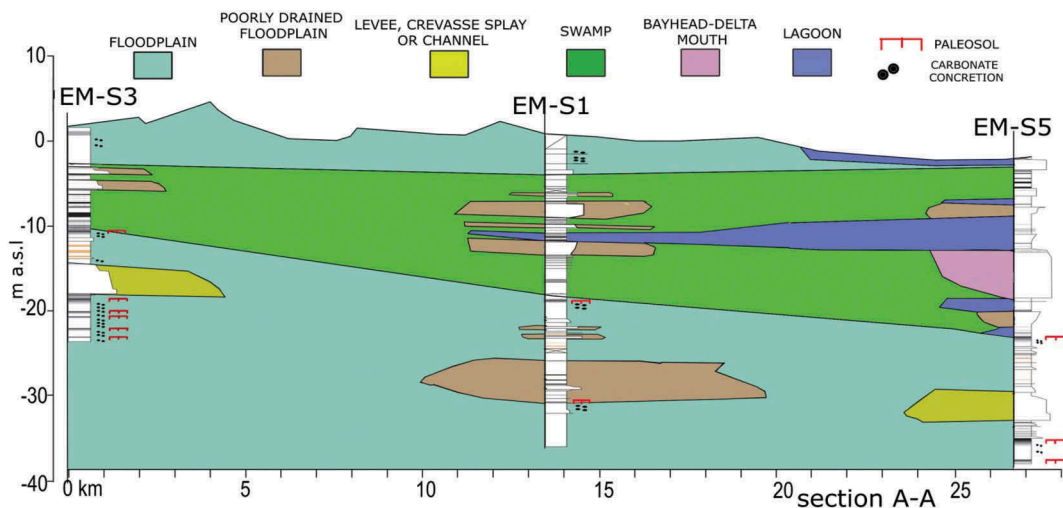


Figure 2. Stratigraphic architecture with indication of the different facies association along section A-A in Figure 1.

lagoonal and bay-head delta deposits. Below the Holocene succession, Pleistocene deposits are predominantly well-drained floodplain silts and clays with subordinate fluvial-channel deposits (Amorosi et al, 2017).

## 2 PALEOSOL ORIGIN AND DEVELOPMENT

The floodplain facies association is characterized by the presence of paleosols, buried ancient soils formed on a ground surface of the past and subjected to physical, biological and chemical modifications caused by the interactions between soil, atmosphere and vegetation. Their development is strictly connected to fluvial activity which in turn depends on river sediment supply/discharge. A schematic representation of paleosol horizons ( $A_b$ ,  $B_k$ ,  $B_w$ ) development is shown in Figure 3. When fluvial incision takes place in response to eustatic or climatic control, the adjacent interfluvial areas are prevented from river flooding and they experience soil development (paleosol 1 in Figure 3 top). In case of prolonged subaerial exposure, vegetation starts to grow on the top soil, enriching the  $A_b$  horizon in organic matter. Moreover, weathering in the vadose zone causes leaching of carbonates from horizon  $A_b$  and their precipitation into the underlying  $B_k$ , in form of millimetric to centimetric nodules. The horizon  $B_w$  is characterized by incipient weathering, while horizon C does not experience pedogenetic modifications. In case of high sediment supply/discharge, fluvial incision is rapidly filled by the transported sediments, and interfluvial areas experience frequent flooding events and crevasse lobe accumulation. Under these conditions, the water table is usually

close to the ground level and then, there is no vadose zone. Due to the fact that river continues to supply new sediments, soil formation is hindered. When the river enters a new stable phase of bed incision, renewed pedogenesis occurs on the interfluvial areas (paleosols 2 and 3 in Figure 3 top).

Holocene paleosols are more discontinuous and immature (Entisols, Amorosi et al., 2014). Paleosol identification is a valid help in the stratigraphic analysis of mud-dominated Late Pleistocene and Holocene deposits. For this reason, they are largely used as regional stratigraphic markers (Amorosi et al, 2017).

## 3 PALEOSOL IDENTIFICATION

In current practice, paleosols in floodplain deposits can be identified by the physical analysis of core samples (visual inspection). The  $A_b$  horizon usually exhibits a darker colour with respect to the illuvial  $B_k$  -  $B_w$  horizons, due to the higher quantity of organic matter. The  $B_k$  horizon typically shows carbonate nodules and often a microstructure created by calcareous cementation between particles. Figure 3 (bottom) shows a typical succession of horizons  $A_b$ - $B_k$ - $B_w$ . Considering the results of the pocket penetrometer, represented in Figure 4 for the EM-S3 borehole, it can be observed that  $A_b$  (whose top is identified with the paleosol symbol shown in the legend, just below the poorly drained floodplain) shows higher values of pocket penetrometer (PP) due to its overconsolidation state created by aging and pedogenetic processes, while  $B_k$  is characterized by medium-high values of PP, as a result of the carbonate accumulation and/or of the calcareous cementation between solid particles. In addition to the visual core inspection, simple

#### 4 ROBERTSON'S CLASSIFICATION CHARTS

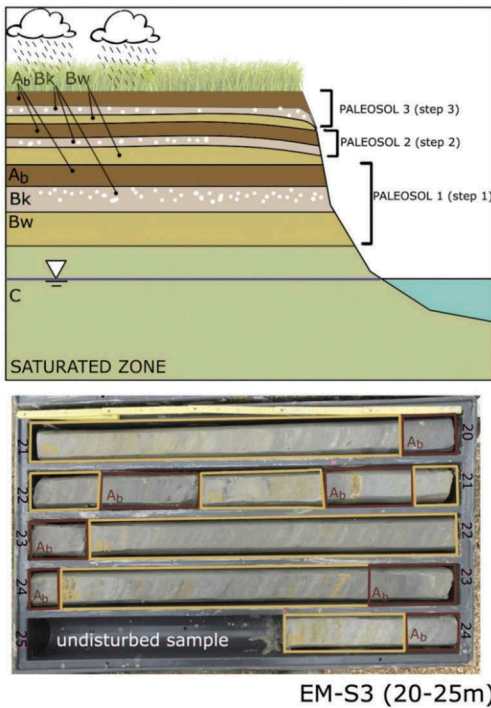


Figure 3. Top: schematic representation of development of paleosol horizons ( $A_b$ ,  $B_k$ ,  $B_w$ ). Bottom: picture of the cores extracted at 20 and 25m depth from EM-S3 borehole.

laboratory tests have been performed in order to control experimental data that characterize the paleosols stratigraphy (Bruno et al, 2020).

In Figure 4, standard characterization tests have been performed on two samples of the  $A_b$  horizon of core EM-S3 (11.55m and 19.55m), on one sample of the  $B_k$  horizon (12.55m) and two samples of the C horizon (20.55m and 14.35m). The carbonate content showed low values (close to zero) for the  $A_b$  samples. The organic content determination confirmed that the highest values belong to the  $A_b$  horizon, which is coherent with the presence of a vegetation cover during soil development. An increase in particle grain size was observed from paleosol horizon  $A_b$  to  $B_k$  at the depth of 11.50-12.50 m. Indeed, the deposition in the  $B_k$  horizon of Fe and Mn oxides and the formation of secondary calcite nodules causes the enrichment in coarse grain material (recognized as sand in the laboratory procedure). On the other hand, the plasticity index is greater in the  $A_b$  horizon. A likely explanation is accumulation and mineralization of the organic matter and its association with clay minerals (Bruno et al, 2020). Samples from C horizons, not subjected to pedogenic processes, show an organic content close to 2.3%,  $PI$  around 16-17%, carbonate content  $\sim 20\%$ , clay content of  $\sim 15\%$  and silt content  $\sim 75\%$ .

The observations of cores, extracted with a continuous perforating system, and, as additional tool, the results of classification tests carried out in the geotechnical laboratory, are a valuable aid for the identification of paleosol horizons in alluvial deposits. These types of investigations require a significant budget, especially when the study involves large areas. The economic effort, as well as the duration of the investigation campaign, could be significantly reduced by means of other geotechnical in situ tests. To this scope, CPTs, being rapid, cost-effective and widely used in practice, are taken into account as a possible additional investigation method, to be used with the aim of extending punctual information from boreholes to larger areas. In this paper, the application of CPT tests is analysed with respect to determination of the soil stratigraphy deduced from the soil behaviour type index (SBT) (Robertson, 2010). Paleosols are geological horizons with peculiar mechanical behaviour due to micro-structure creation as a consequence of pedogenetic processes and aging. A microstructured soil is characterized by a higher yield stress, peak strength and small-strain stiffness  $G_o$  with respect to an ideal soil. At large strain, the soil is subjected to destructuration and it may show a contractive behaviour (Leroueil and Hight, 2003). In order to investigate the effectiveness of this approach, the well-drained floodplain deposits identified in the three CPTU profiles, close to EM-S1, EM-S3 and EM-S5, were plotted on different soil classification charts available in the literature. Firstly, the Robertson (1990) chart was considered (Figure 5). Potentially, CPT-based charts could have the capability of recognizing paleosols since they rely on in situ mechanical behaviour and not directly on soil classification criteria based on grain size distribution and plasticity, such as the USCS (Unified Soil Classification System) (Tonni et al., 2019a, Tonni et al., 2019b). On the normalized  $Q_r-F_r$  chart the majority of records belong to SBT zone 3 (clay), on the right side of the normal consolidated central area, characterized by increasing  $OCR$ .

Data which have CPT-based SBT in either zone 4 or 5, could reflect the same soil (in terms of grain size), but stiffer, with higher  $OCR$  (horizon  $A_b$ ), or a coarser layer as a consequence of a higher percentage of sand or carbonate nodules ( $B_k$  horizons). Similar results can be deduced from the  $Q_r-B_q$  charts (lower part of Figure 5), where the majority of the points are located in zone 3 (clay) and, to a lesser extent, in zones 4 (silty mixtures) and 5 (sand mixtures). Points showing SBT 4 and 5 plot around the vertical line  $B_q=0$ . Comparing these groups of data (SBT 4 and 5) in the  $Q_r-F_r$  and  $Q_r-B_q$  charts, it can be noticed that a larger amount of points plots into zones 4 or 5 in the  $Q_r-B_q$  chart rather than in the  $Q_r-F_r$  chart. This likely reflects the presence of a significant silty component in this part of the deposits (see also grain size distribution in Figure 4 of samples EM-S3 and its

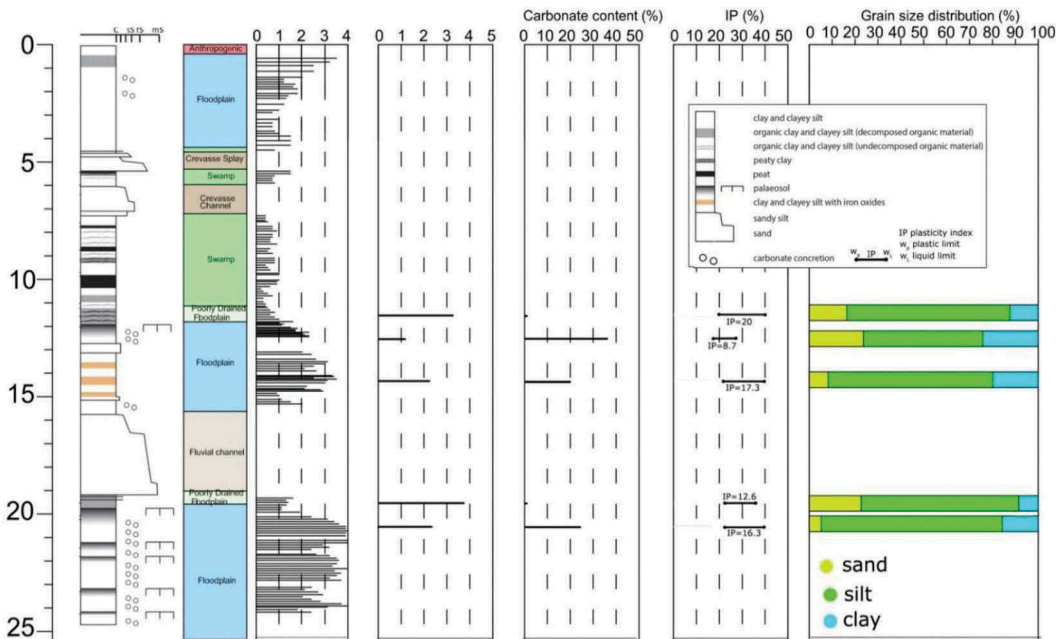


Figure 4. Physical characterization of five soil samples belonging to the continuous coring EM-S3. Two samples (11.55 and 19.55m deep, respectively) belong to horizon  $A_b$ ; The sample at 12.55m belong to horizon  $B_k$  and the remaining two samples belong to horizon C.

Robertson's chart in Figure 5). These layers can be more effectively detected using the  $B_q$  parameter, which captures the dilatant behavior of silts (or paleosols) and the possible occurrence of coarser thin layers, not revealed by  $F_r$ . In a recent update of the classification charts, Robertson (2016) suggested to use  $CD=70$  line in the  $Q_{tn}-F_r$  chart (Figure 5) to recognize microstructured soils. Indeed, the  $CD=70$  line should separate contractive from dilatative behaviours and it can be expressed with the following formula:

$$CD = 70 = (Q_m - 11)(1 + 0.06 F_r)^{17} \quad (1)$$

With  $Q_m$  normalized cone resistance and  $F_r$  normalized friction ratio.

In case of microstructured soils with contractive behaviour at large strains, but due to the increased strength and stiffness for cementation or aging, higher values of  $Q_m$  may be recorded. As a result, cemented soils wrongly plot on the dilatative region of the chart. In Figure 5 the majority of the points plots below the boundary line  $CD=70$  and only few points, that may show some microstructure, above it. On the  $Q_m-F_r$  chart, the modified SBT<sub>n</sub> boundaries (black continuous lines) proposed by Schneider et al (2012) have been superimposed on the original SBT<sub>n</sub> zones (black dashed lines) by Robertson (1990). The modified contours are based on the Modified Soil Behaviour Index  $I_B$  expressed as follows:

$$I_B = 100 \frac{(Q_m + 10)}{(Q_m F_r + 70)} \quad (2)$$

In addition to Robertson's approaches, a different classification system, proposed by Schneider et al (2008) was also taken into account. Its application showed that the investigated soils have a predominantly contractive behaviour, belonging to the clay like contractive soils (CC) and the transitional contractive soils (TC). Schneider et al (2008) also suggests that microstructured soils plot above a line of equation  $Q_m = -U_2 + 20$ , where  $U_2$  is defined as the ratio between the excess pore water pressure and the effective stress in the point. No points that satisfy this condition were found within the investigated depth. Figure 6 shows the results of the CPTU test performed in close proximity to EM-S5, in terms of corrected cone resistance  $q_r$ ,  $f_s$  and  $u_2$ . Using the sedimentological characterization of facies in core EM-S5, and the SBT classification system, the geological-geotechnical stratigraphy was identified. It can be easily observed that the recognition of the different sedimentary facies starting solely from CPTU classification, in case no geological information is available, is not straightforward, as clearly shown by the comparison between central lagoon, crevasse splay and floodplain deposits. Focusing on the alluvial plain deposit (floodplain), it is interesting at this stage to compare how points plot with depth in the classification charts (Figure 6). The comparison

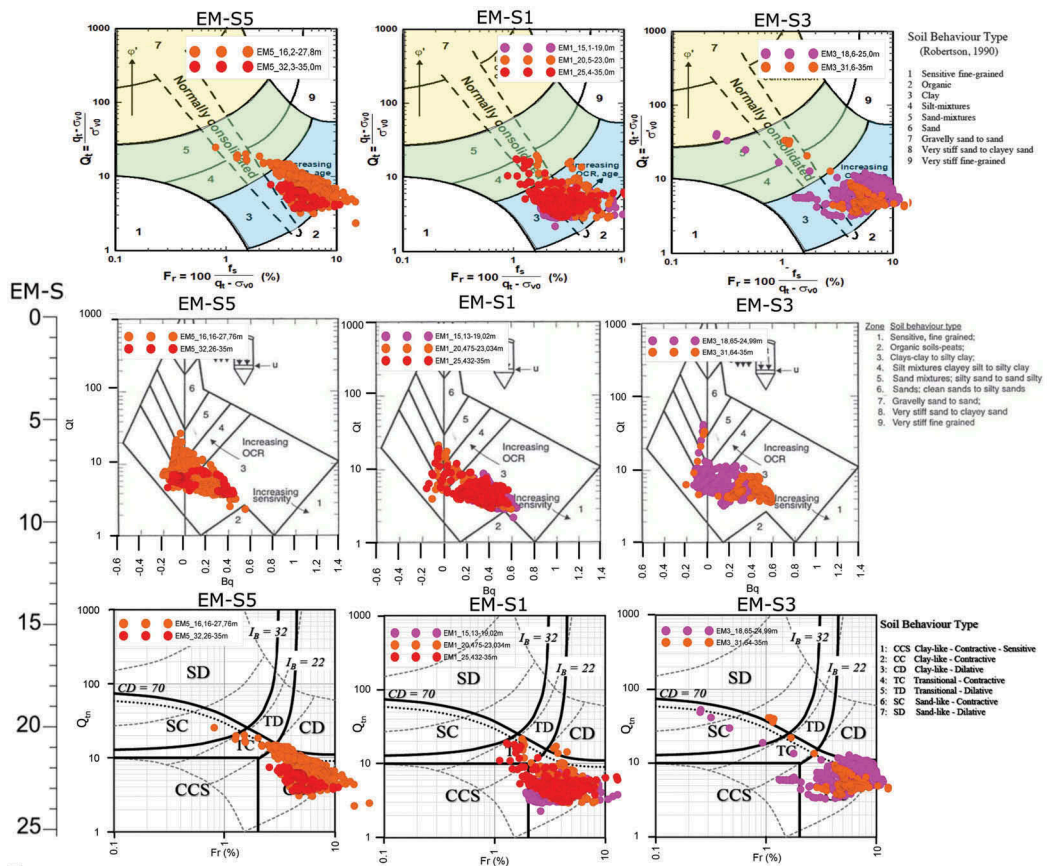


Figure 5. Soil Behaviour Type data plotted in the Robertson (1990)  $F_r-Q_r$ , and  $B_q-Q_r$  charts and in Robertson (2009)  $F_r-Q_{rn}$  chart for the floodplain deposits identified in EM-S5, EM-S1 and EM-S3 boreholes.

suggests that crevasse splay horizons, in particular those at a depth of 18 – 19.5 m and 22.5 – 23 m, show SBT 4 and 5 in almost all types of charts. This is due to the presence of cm-thick sandy layers that characterize this type of facies. On the contrary, the floodplain layers, where paleosol horizons have been identified, plot in SBT zone 4 only on the  $Q_r-B_q$  Robertson (1990)'s chart, while the other classification charts recognize them as homogeneous SBT 3. This peculiarity could be justified by the fact that in fine grained soils the  $B_q$  parameter is more sensitive than  $F_r$ , to the presence of structure variations within thin layers, which cannot be detected through the  $F_r$  parameter.

## 5 CONCLUSIONS

In this paper, it has been shown how CPT data collected in floodplain deposits of the river Po plot on well-known classification charts (Robertson 1990; Robertson, 2009, Schneider et al, 2008).

Although CPTU classification charts proved to be a potential valuable help in the identification of

sedimentary facies in the alluvial Po Plain, they do not provide univocal identification of paleosol horizons without the support of their geological preliminary recognition. This evidence applies to low mature paleosols, peculiar horizons of the floodplain facies subjected in the past to microstructuration for cementation ( $B_R$ ) or aging ( $A_b$ ): they do not appear to be easily identified by using only information from cone penetration tests ( $q_p$ ,  $f_s$ ,  $u_2$ ). Integrating the visual inspection of paleosols from cores with basic classification laboratory tests is crucial to a correct geotechnical-geological interpretation, especially in relatively homogeneous, mud-prone alluvial deposits, where sand bodies display strongly lenticular geometries.

The paleosol horizons investigated in this study cannot be identified as microstructured soils in the classification charts available in the literature. This fact is probably a sign of the low maturity of these paleosols (Inceptisols), which only account for relatively short periods of subaerial exposure of the ancient topsoil. Nonetheless, a characteristic feature of paleosol horizons seems to be shown by the  $Q_r-B_q$  Robertson's (1990) chart, which

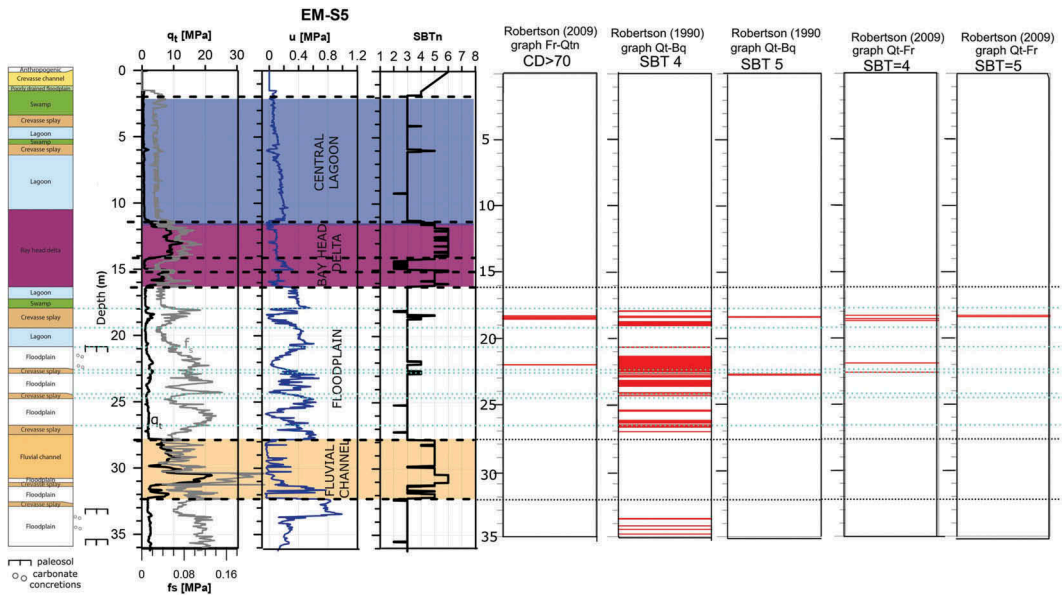


Figure 6. Left side: stratigraphic log of the continuous coring EM-S5. From left to right: corrected tip resistance  $q_t$ , sleeve friction  $f_s$ , pore water pressure  $u_2$  and soil behaviour type (Robertson, 2009) vs depth of the CPTU performed in close proximity to EM-S5. The final five columns represent with a red line the depth where SBT 4 or 5 have been found in the classification charts.

highlights the presence of SBT 4, where all the other charts provide SBT 3. Further investigations through dilatometer or other in situ tests will be carried out in the next future to expand the results of this study.

## REFERENCES

- Amorosi, A., Bruno, L., Campo, B., Morelli, A., Rossi, V., Scarponi, D., Hong, W., Bohacs, K.M., Drexler, T.M. 2017. Global sea-level control on local parasequence architecture from Holocene record of the Po Plain, Italy. *Marine and Petroleum Geology*.
- Amorosi, A., Bruno, L., Rossi, V., Severi, P., Hajdas, I. 2014. Paleosol architecture of a late Quaternary basine margin sequence and its implications for high resolution, non-marine sequence stratigraphy. *Glob. Planet. Change* 112:12–25.
- Bruno L., Marchi M., Bertolini I., Gottardi G., Amorosi A. 2020. Climate control on stacked paleosols in the Pleistocene of the Po Basin (northern Italy). *Journal of Quaternary Science*, vol 35(4): 559–571.
- Leroueil, S. & Hight, D.W. 2003. Behaviour and properties of natural soils and soft rocks. In Tan et al (eds), *Characterization and engineering properties of natural soils*, vol.1.
- Robertson, P.K. 2016. Cone penetration test (CPT)-based soil behaviour type (SBT) classification system-an update. *Canadian Geotechnical Journal*.
- Robertson, P.K. 1990. Soil classification using the cone penetration test. *Canadian Geotechnical Journal*, 27(1): 151–158.
- Robertson, P.K. 2009. Interpretation of cone penetration test-a unified approach. *Canadian Geotechnical Journal*, 46(11): 1337–1355.
- Schneider, J.A., Randolph, M.F., Mayne, P.W., Ramsay, N. R. 2008. Analysis of factors influencing soil classification using normalized piezocone tip resistance and pore pressure parameters. *Journal of Geotechnical and Geoenvironmental Engineering*, 134(11): 1569–1586.
- Schneider, J.A., Hotstream, J.N., Mayne, P.W., Radolph, M. F. 2012. Comparing CPTU Q-F and  $Qt-\Delta u/2/6'$  soil classification charts. *Geotechnique Letters* 000:1–7.
- Tonni, L., Garcia Martinez, M.F., Maurini, D., Calabrese, L. 2019a. Developing a regional-scale geotechnical model of the north-western Adriatic coastal area (Italy) for urban planning and robust geotechnical design. *Proc. 17th European Conference on Soil Mechanics and Geotechnical Engineering, ECSMGE*.
- Tonni, L., Garcia Martinez, M.F., Rocchi, I. 2019b. Recent developments in equipment and interpretation of cone penetration test for soil characterization. *Rivista Italiana di Geotecnica* 53(1): 71–99.